



## MINIREVIEW

[View Article Online](#)  
[View Journal](#) | [View Issue](#)Cite this: *Chem. Sci.*, 2020, **11**, 10605

All publication charges for this article have been paid for by the Royal Society of Chemistry

## Light opens a new window for N-heterocyclic carbene catalysis

Jing Liu,<sup>a</sup> Xiao-Ning Xing,<sup>b</sup> Jin-Hai Huang,<sup>a</sup> Liang-Qiu Lu <sup>\*a</sup> and Wen-Jing Xiao <sup>\*a</sup>

N-Heterocyclic carbenes (NHCs) are efficient Lewis basic catalysts for the umpolung of various polarized unsaturated compounds usually including aldehydes, imines, acyl chlorides and activated esters. NHC catalysis involving electron pair transfer steps has been extensively studied; however, NHC catalysis through single-electron transfer (SET) processes, despite having the potential to achieve chemical transformations of inert chemical bonds and using green reagents, has long been a challenging task in organic synthesis. In parallel, visible-light-induced photocatalysis and photoexcitation have been established as powerful tools to facilitate sustainable organic synthesis, as they enable the generation of various reactive radical intermediates under extremely mild conditions. Recently, a number of elegant visible-light-induced, NHC-catalyzed transformations were developed for accessing valuable organic compounds. As a result, this minireview will highlight the recent advances in this field.

Received 30th June 2020

Accepted 8th August 2020

DOI: 10.1039/d0sc03595e

[rsc.li/chemical-science](http://rsc.li/chemical-science)

## 1. Introduction

N-Heterocyclic carbenes (NHCs) are a class of intriguing nitrogen-containing heterocyclic compounds possessing a bivalent carbon atom with six valence electrons.<sup>1</sup> According to their general properties and applications in modern chemistry, NHCs are approximately categorized into three sections: (i) ligands for transition metals; (ii) coordination to *p*-block elements and (iii) organocatalysts. Since the early 2000s, NHCs have been employed extensively as powerful and efficient nucleophilic or Brønsted base catalysts<sup>2</sup> for chemical bond formations, including cross-benzoin reactions, Stetter reactions, cycloadditions and so on. Several comprehensive reviews have summarized these important advances.<sup>3</sup> However, most of these investigations presumably involved electron pair transfer steps. With nucleophilic NHC catalysis as an example, the majority of these processes are initiated by nucleophilic attack of the carbene catalyst on the carbonyl group. Subsequently, the generated Breslow intermediate, homoenolate or dienolate, usually reacts with strong electrophiles with  $sp^2$  carbon, such as active ketones and imines. Weak electrophiles with  $sp^3$  carbon, such as alkyl halides, are inert in NHC-catalyzed reactions. In contrast to electron pair transfer pathways, the development of NHC-catalyzed reactions through single-electron transfer (SET) processes is still in its infancy.<sup>4</sup> Although Fukuzumi and co-workers carefully studied the redox or electron transfer

characteristics of Breslow intermediates in the late 1990s,<sup>5</sup> it wasn't until 2008 that Studer and co-workers reported pioneering work on the biomimetic, carbene-catalyzed oxidation reaction of aldehydes, which involves two successive single-electron oxidations of the Breslow intermediate by 2,2,6,6-tetramethyl-1-piperidinyloxy (TEMPO).<sup>6</sup> After that, Rovis,<sup>7</sup> Chi<sup>8</sup> and Ye<sup>9</sup> demonstrated that single-electron oxidations of NHC-bound intermediates are indeed useful for developing new chemical transformations. However, these studies are primarily limited to specific oxygen or functionalized carbon-centred radicals. In 2019, Nagao and Ohmiya developed an NHC-catalyzed decarboxylative alkylation of aldehydes using redox-active esters.<sup>10a</sup> Soon after, the same catalysis strategy was applied to two three-component coupling reactions *via* a radical relay process.<sup>10b,c</sup> Despite these substantial contributions, there are still only limited radical reactions that take place through single NHC catalysis.

Over the past decade, a wide range of visible-light-induced organic photochemical reactions have been successfully explored to meet the requirement of green synthetic chemistry.<sup>11</sup> Key to these successes is the use of the strategy of visible light photocatalysis to generate highly reactive radical species under environment- and user-friendly conditions. In addition, nature always inspires synthetic chemists to mimic its multi-enzymatic systems for constructing molecular complexity.<sup>12</sup> In this context, the combination of photocatalysis with other catalytic modes,<sup>13</sup> including NHC catalysis, has been established as an important platform for modern green synthesis. This distinct catalysis mode could generate products with remarkable selectivity, which are inaccessible through a single NHC catalyst system. This minireview focuses on recent

<sup>a</sup>Key Laboratory of Pesticide & Chemical Biology, Ministry of Education, College of Chemistry, Central China Normal University, 152 Luoyu Road, Wuhan, Hubei 430079, China. E-mail: [luliangqiu@mail.ccnu.edu.cn](mailto:luliangqiu@mail.ccnu.edu.cn); [wxiao@mail.ccnu.edu.cn](mailto:wxiao@mail.ccnu.edu.cn); Web: <http://chem-xiao.ccnu.edu.cn>

<sup>b</sup>Anyang Academy of Agricultural Sciences, 833 Wenming Road, Anyang, Henan, China

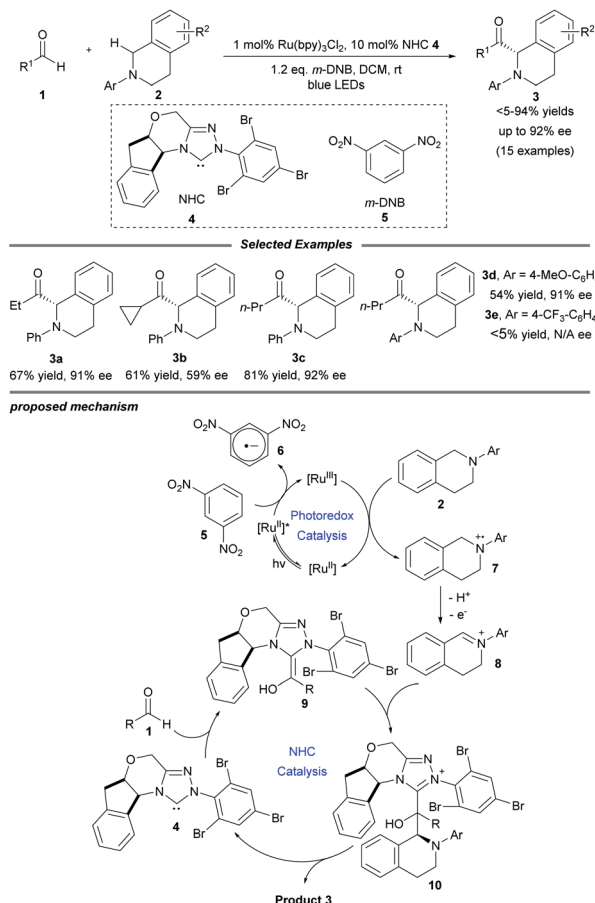
advances in visible-light-induced, NHC-catalyzed organic reactions, in which light is used to excite the additional photosensitizer (photoredox catalysis mechanism) or the NHC-bound intermediate itself (direct photoactivation mechanism).

## 2. Synergistic NHC/photoredox catalysis

In recent years, synergistic NHC/photoredox catalysis has been used to realize several significant organic transformations under oxidative and neutral conditions. In these dual catalysis systems, an independent NHC catalyst is used for umpolung of carbonyls *via* the formation of Breslow intermediates or transient acyl azoliums. In parallel, a photocatalyst (PC) is employed to absorb visible light and the excited photocatalyst can promote the generation of highly reactive radical species *via* SET events with substrates (Fig. 1a) or NHC-intermediates (Fig. 1b). Compatibility between these two catalysts is crucial to make sure these radical reactions proceed well with remarkable efficiency and selectivity.

### 2.1 Visible-light-driven oxidative reactions

In 2012, Rovis and co-workers first reported that photoredox catalysis can be combined with chiral NHC catalysis, realizing the catalytic asymmetric acylation of *N*-aryl tetrahydroisoquinolines with aldehydes by using an aminoindanol-derived NHC catalyst and a Ru(bpy)<sub>3</sub>Cl<sub>2</sub> photocatalyst (Scheme 1).<sup>14</sup> In this process, using a sub-stoichiometric quantity of the weak organic oxidant *meta*-dinitrobenzene (*m*-DNB) is essential for obtaining high reaction efficiency. Stronger oxidants such as BrCCl<sub>3</sub> may result in oxidative decomposition of the NHC catalyst. A series of aliphatic aldehydes and tertiary amines participate smoothly in this transformation, affording the corresponding  $\alpha$ -amino ketones in good yields and excellent stereoselectivities. Notably, sensitive functionalities such as olefins, thioethers and esters were well tolerated. However, electron-donating substituents on the *N*-aryl group are essential for



Scheme 1 Photo/NHC-cocatalyzed enantioselective acylation of *N*-aryl tetrahydroisoquinolines with aldehydes. bpy: 2,2'-bipyridine.

this reaction in order to reduce the competing radical dimerization.

Mechanistically, Ru(bpy)<sub>3</sub><sup>3+</sup> is generated upon the oxidative quenching of excited \*Ru(bpy)<sub>3</sub><sup>2+</sup> by *m*-DNB accompanied by the release of arene radical anion 6. Then tetrahydroisoquinoline 2 is oxidized by the Ru(bpy)<sub>3</sub><sup>3+</sup> to form amine radical cation 7, followed by release of a proton and an electron to deliver the iminium ion species 8. Meanwhile, NHC catalyst 4 reacts with aliphatic aldehyde 1 to generate the activated Breslow intermediate 9. Stereoselective addition of this nucleophilic intermediate to iminium ion 8 leads to the formation of a C–C bond to yield aminoalcohol derivative 10. Finally, the enantio-enriched  $\alpha$ -amino ketone product 3 is obtained and the NHC catalyst is regenerated by the following elimination of adduct 10, and the NHC catalytic cycle is then completed.

In 2018, Miyabe and co-workers disclosed a facile protocol for oxidative esterification of cinnamaldehydes by using the strategy of NHC/photoredox dual catalysis (Scheme 2).<sup>15</sup> A series of methyl cinnamates bearing electron-donating or -withdrawing groups were obtained under mild conditions. In addition, 2-naphthaldehyde could also undergo this transformation smoothly and be converted into the corresponding ester 12d. A stoichiometric amount of the external oxidant BrCCl<sub>3</sub> is necessary to prevent reduction of the C=C bond. The

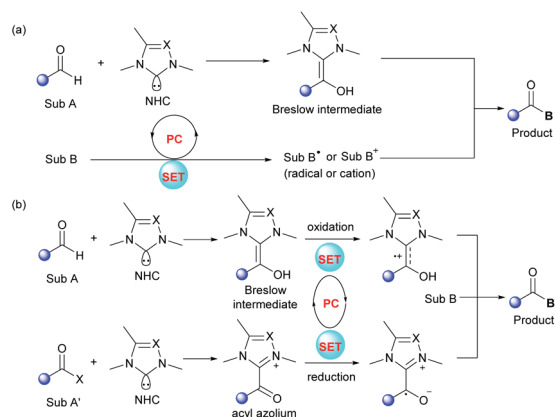
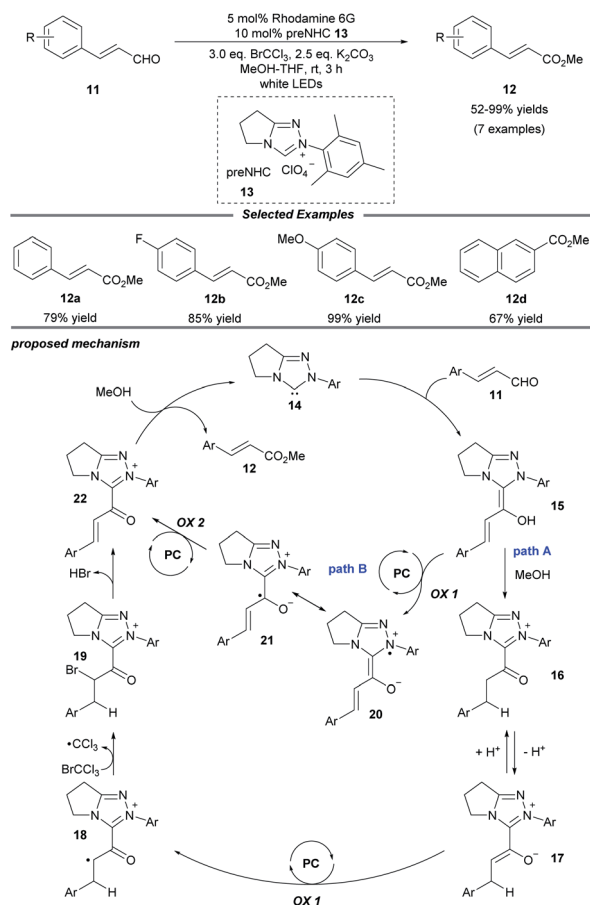


Fig. 1 Two representative activation modes of synergistic NHC/photoredox catalysis.

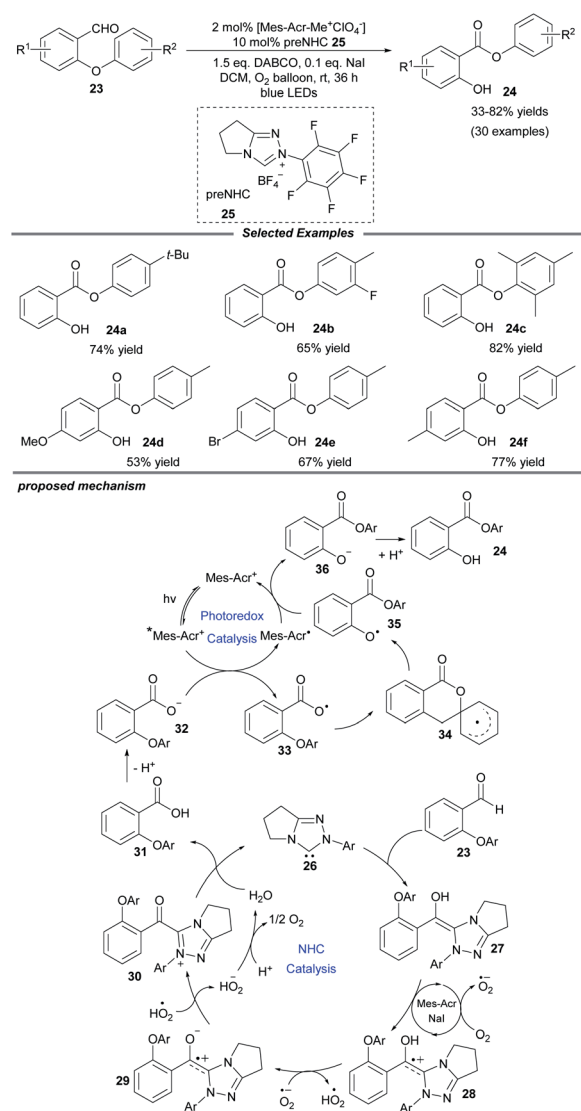




Scheme 2 Photo/NHC-cocatalyzed oxidative esterification of cinnamaldehyde derivatives.

mechanism initiates with the interaction of the NHC with the aldehyde to form the Breslow intermediate 15. In path A, subsequent protonation of 15 by MeOH leads to the enolate ion pair 17 through a stable azolium intermediate 16. Then, a SET oxidation of enolate 17 by the excited-state organophotocatalyst rhodamine 6G delivers a radical cation 18, which reacts with  $\text{BrCCl}_3$  to generate the brominated cation intermediate 19. Then a resonance-stabilized cation 22 is obtained *via* the elimination of HBr. Ultimately, cation 22 reacts with MeOH to provide the ester product 12 and regenerate the NHC catalyst 14. In another possible pathway (path B), acylium ion equivalent 22 can be delivered through two consecutive photocatalytic SET oxidations of Breslow intermediate 15.

Molecular oxygen is a beneficial and green oxidant in chemical oxidation reactions. Quite recently, Ye and colleagues documented an NHC/photo-cocatalyzed, aerobic oxidative Smiles rearrangement of *o*-aryl salicylaldehydes for the preparation of aryl salicylates (Scheme 3).<sup>16</sup> With the use of an achiral triazolium preNHC catalyst and the Fukuzumi photocatalyst, aryl groups with different electronic properties migrate well in the rearrangement process. NaI is a prerequisite additive to accelerate the electron transfer. A series of control experiments show that the Breslow intermediate is oxidized by molecular oxygen in the presence of NaI and acridium salt. A plausible



Scheme 3 Photo/NHC-cocatalyzed oxidative Smiles rearrangement. DABCO: 1,4-diazabicyclo[2.2.2]octane.

catalytic cycle is proposed in Scheme 3. The attack of NHC 26 on salicylaldehyde generates the key Breslow intermediate 27, which can be oxidized by  $\text{O}_2$  through a SET process. Subsequent deprotonation of the generated intermediate 28 by a superoxide anion affords a zwitterionic radical species 29 and a hydroperoxide radical, which can further oxidize 29 to deliver acyl azolium 30. Then the acyl azolium undergoes a hydrolysis process to furnish the salicylic acid 31, completing the oxidative NHC catalytic cycle. Meanwhile, photoexcitation of the acridium salt by visible light affords the excited photocatalyst,  $[\text{Mes-Acr}^+]^*$ , which can undergo reductive quenching by the carboxylic anion 32 to give carboxyl radical 33 and an Acr-Mes radical. Following this, the intramolecular Smiles rearrangement generates the oxygen radical 35 through a spirocyclic radical intermediate 34. Then the oxygen radical oxidizes the Acr-Mes radical to regenerate the photocatalyst and form the oxygen anion species 36, which undergoes protonation to yield the desired product 24.

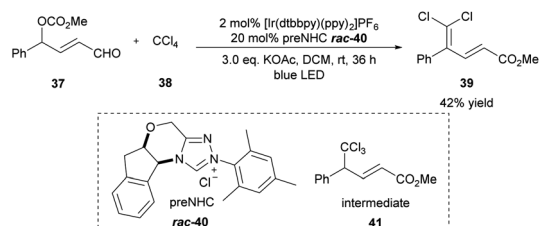


## 2.2 Visible-light-driven redox neutral reactions

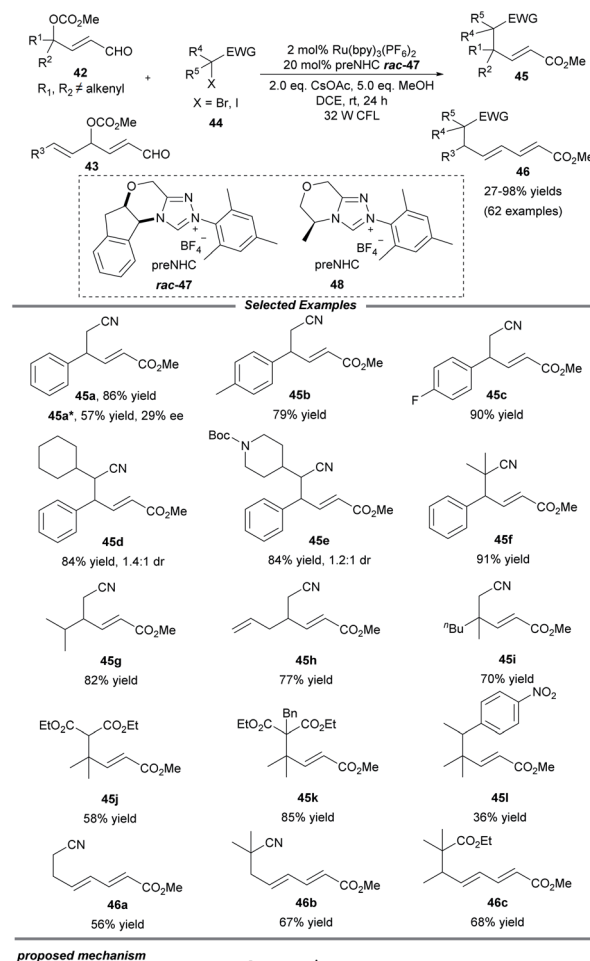
The dihalomethylene group widely occurs in natural products and biologically active molecules.<sup>17</sup> In 2016, the Sun group described one example of the  $\gamma$ -dichloromethylenation method by employing [Ir(dtbbpy)(ppy)]PF<sub>6</sub> as the photoredox catalyst and triazolium salt **40** as the NHC precatalyst (Scheme 4).<sup>18</sup> Under the irradiation of a blue LED light, the unsaturated  $\delta,\delta$ -dihalo ester product **39** was generated from aldehyde **37** and CCl<sub>4</sub> with a perfect regioselectivity in 42% yield. Presumably, the initial trichloromethylation product **41** is the key intermediate, which could be formed during the cocatalyzed process and undergo elimination of HCl to give the final product. The authors observed that the reaction yield can be further improved by using the more labile radical precursors CBr<sub>4</sub> and CCl<sub>3</sub>Br even without additional light irradiation.

Later in 2019, Ye and co-workers realized an NHC/photoredox dual catalytic protocol for  $\gamma$ - and  $\varepsilon$ -alkylations of enals, affording multisubstituted unsaturated esters with good efficiency and exclusive regioselectivity (Scheme 5).<sup>19</sup> Under mild conditions, this method showed a good substrate scope and functional group compatibility for both constituents. Comfortingly,  $\gamma$ -dialkylated enals could also be tolerated and the desired products containing all-carbon quaternary centers, which are a challenging topic in organic synthesis, could be obtained in moderate to good yields. Notably, a series of primary, secondary and tertiary radical precursors all worked well for this transformation. Through a trienolate intermediate, the  $\varepsilon$ -functionalization of enals **43** that bear alkenyl substituents at the  $\gamma$ -position was also established. Beyond that, a catalytic enantioselective alkylation was examined and a promising enantioselectivity with 29% ee was afforded when the chiral NHC precursor **48** was employed. It was observed that the alkylation process was inhibited in the absence of light, photocatalyst and NHC catalyst. Quenching experiments with the radical scavenger TEMPO confirmed that the transformation should proceed through an alkyl radical pathway.

For the mechanism, Ye proposed that the excited state  $^*\text{Ru}(\text{bpy})_3^{2+}$  is probably quenched by halide to give alkyl radical **49** and the  $\text{Ru}(\text{bpy})_3^{3+}$  photocatalyst. At the same time, NHC **50** reacts with peroxidized enal **42** to deliver the dienolate intermediate **51**, which can be captured by alkyl radical **49** to furnish the homoenolate radical **52**. The oxidation of radical **52** by  $\text{Ru}(\text{bpy})_3^{3+}$  reforms  $\text{Ru}(\text{bpy})_3^{2+}$  and generate the acyl azolium intermediate **53**, followed by attack by MeOH to obtain the final product **45** and close the NHC catalytic cycle.



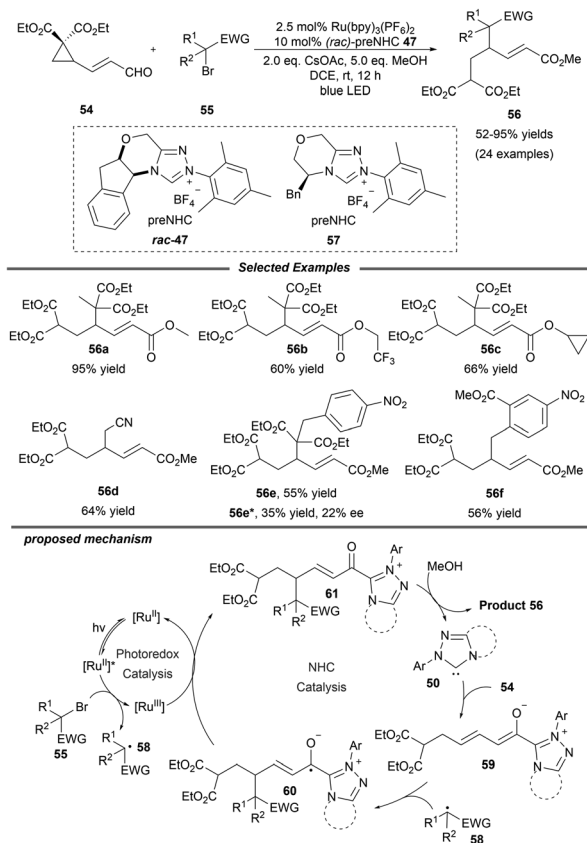
Scheme 4 Photo/NHC-cocatalyzed  $\gamma$ -dichloromethylenation of enal. ppy: 2-phenylpyridine, dtbbpy: 4,4-di-*tert*-butyl-2,2'-bipyridine.



Scheme 5 Photo/NHC-cocatalyzed  $\gamma$ - and  $\varepsilon$ -alkylations of enals with alkyl radicals.

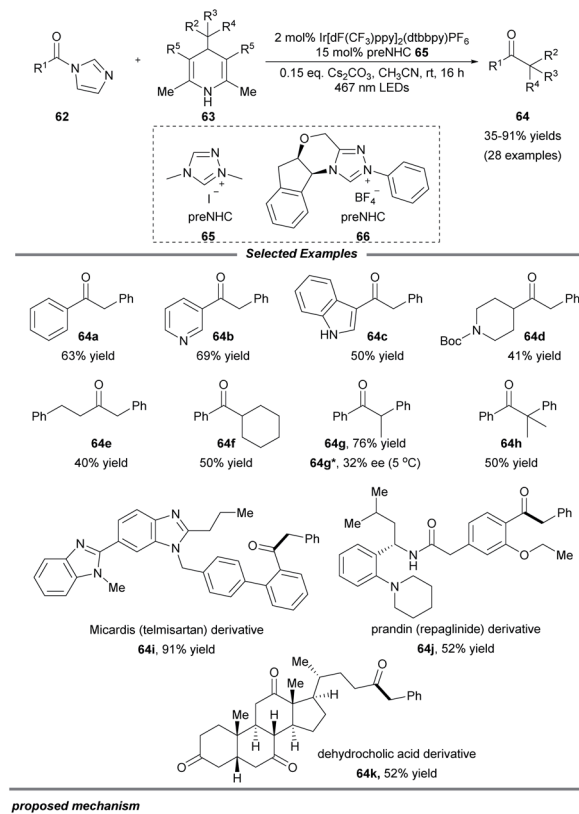
Shortly afterwards, the same group extended this photo/NHC dual catalysis system to the ring opening/ $\gamma$ -alkylation reaction of cyclopropane enal **54** (Scheme 6).<sup>20</sup> A radical-trapping experiment with TEMPO suggests that an alkyl radical relay process is involved. Under mild conditions, a variety of alcohols and halogenated alkylation reagents participate smoothly in this reaction, furnishing the corresponding  $\gamma$ -alkylated  $\alpha,\beta$ -unsaturated esters with moderate to excellent yields. The authors also pointed out that epoxy enals were not suitable for this transformation. Notably, a preliminary asymmetric variant was also studied with enal **54** and  $\alpha$ -benzyl- $\alpha$ -bromomalonate as the substrates by using the chiral NHC precursor **57**, affording



Scheme 6 Ring opening and  $\gamma$ -alkylation of cyclopropane enal.

the product **56e** in a promising enantioselectivity with 22% ee. Mechanistically, NHC **50** reacts with  $\gamma$ -cyclopropane enal **54** to give the dienolate intermediate **59**, which can be trapped by radical **58** which is generated from the alkyl halide *via* photoredox catalysis. The afforded homoenolate radical **60** undergoes a subsequent SET oxidation and alcoholysis to regenerate the NHC catalyst and provide the final product **56**.

Very recently, Scheidt and coworkers realized an elegant single-electron alkylation reaction of acyl azoliums for the synthesis of ketones from carboxylic acids (Scheme 7).<sup>21</sup> Semi-high-throughput experimentation (HTE) facily showed that a Hantzsch ester served as a suitable alkyl radical precursor and acyl imidazole was a suitable azolium radical precursor. This reaction employing 2 mol% iridium photocatalyst and 15 mol% azolium precatalyst exhibits a broad scope for both coupling partners. A series of functional groups, *e.g.*, vinyl, alkynyl, ester, and heteroaryl motifs, were well tolerated. Additionally, to illustrate the ease and practicality of this NHC/photoredox cocatalyzed methodology, the authors also achieved the one-step late-stage functionalization of three carboxylic acid-containing pharmaceutical compounds, producing the desired ketone compounds in moderate to good yields. Notably, when a chiral NHC precursor **66** was used instead of **65**, a promising enantioselectivity of the ketone product **64g** was observed. It is a novel asymmetric acyl-like radical–radical cross-coupling reaction to construct ketones bearing an  $\alpha$ -stereogenic center. A radical trapping experiment with TEMPO proved that

Scheme 7 Alkylation of acyl azoliums for the synthesis of ketones. dF(CF<sub>3</sub>)ppy: 2-(2,4-difluorophenyl)-5-trifluoromethylpyridine.

radical species are involved in this process. The proposed reaction pathway starts from the reductive quenching of excited state  $^*[Ir^{III}]$  by the Hantzsch ester to afford photocatalyst  $[Ir^{II}]$ , together with radical cation species **67** which can undergo fragmentation to form pyridine by-product **68** and alkyl radical **69**. Then acyl triazolium **70**, generated from the acyl imidazole, the NHC precursor and base, undergoes a single-electron reduction to yield the radical intermediate **71** and reform the ground-state photocatalyst  $[Ir^{III}]$ . Finally, radical–radical coupling of intermediates **72** and **69** provides the desired product **64** and releases the NHC catalyst **73**.

### 3. Photoexcited NHC-catalyzed transformations

In addition to the aforementioned dual catalysis, single-NHC-catalyzed radical reactions under UVA or visible light

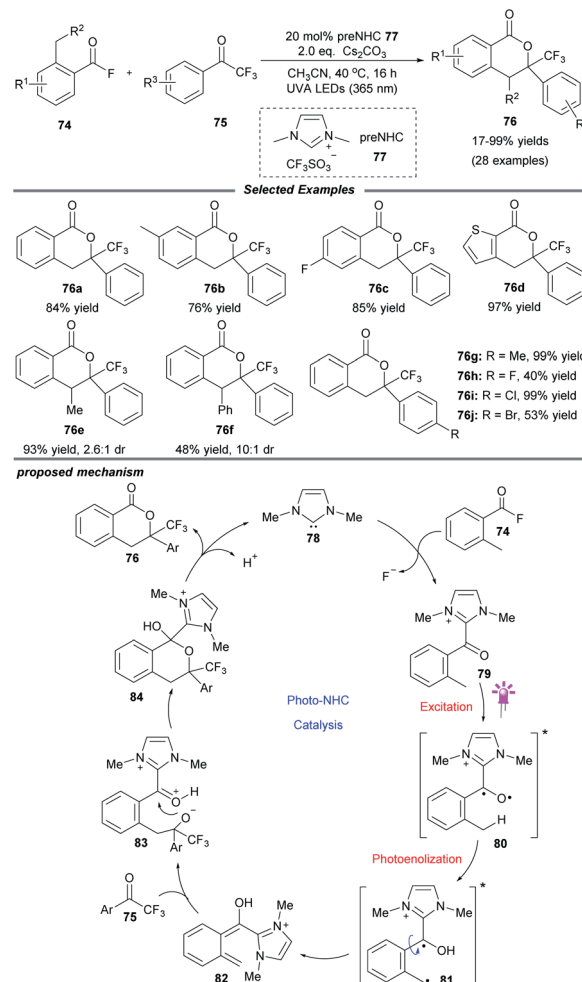


irradiation were also developed. In these transformations, addition of the NHC catalyst to a carbonyl substrate generates an acyl azolium or Breslow intermediate, which can reach an excited state upon irradiation. Following this, these excited species can undergo further transformations through different pathways leading to the final products (Fig. 2a). Also, some  $\alpha$ -diazo carbonyl substrates can absorb light directly and then generate active ketene intermediates, which can be captured by the NHC catalyst to afford enolate species (Fig. 2b).

UVA-light-induced photochemical transformations of aromatic aldehydes and ketones have been well established;<sup>22</sup> however, carboxylic acid substrates are always limited due to their shorter absorbing wavelength than that of the corresponding ketones. To address this issue, in 2019, the Hopkinson group utilized a combination of photoactivation with NHC organocatalysis to accomplish a sequential photoenolization/Diels–Alder (PEDA) reaction of acyl fluorides **74**, resulting in the formation of isochroman-1-one derivatives **76** in moderate to high yields (Scheme 8).<sup>23</sup> It is particularly noteworthy that *o*-ethyl and *o*-benzyl-substituted acid fluorides, which could not be employed to construct isochroman-1-ones by previous NHC-catalyzed methods, successfully participated in this reaction, too. Regrettably, some dienophiles such as isatins or 2-ketoesters failed to furnish the desired product, possibly owing to their competitive absorption of intense UVA light.

The authors proposed a possible mechanism to illustrate this PEDA process. The imidazolylidene IMe **78**, generated *in situ* by deprotonation of the NHC precursor **77** with base, selectively attacks the acyl fluoride, releasing a fluoride anion and giving *o*-toluoyl azolium **79**. This benzophenone-like intermediate can be photoexcited *via* intersystem crossing to generate a triplet excited state **80**, which undergoes intramolecular 1,5-hydrogen atom transfer to afford triplet dienol biradical species **81**. Following rotation, **81** gives rise to a hydroxyl *o*-quinodimethane intermediate **82**, which can react with the ketone to form the cycloadduct **84** *via* the transient species **83**. Finally, the catalytic cycle is completed with the elimination of NHC catalyst **78** and generation of the desired PEDA product **76**.

Soon after, a particularly NHC-catalyzed photooxidation reaction of tetrahydroisoquinoline (THIQ)-tethered aldehydes



Scheme 8 NHC-catalyzed photoenolization/Diels–Alder reaction.

**85** was described by Ye and coworkers (Scheme 9).<sup>24</sup> In this intramolecular cross dehydrogenative coupling process, molecular oxygen was chosen as the optimal oxidant and a catalytic amount of NaI was necessary to improve the efficiency. Substrates with different substituents on the benzaldehyde and THIQ skeletons were compatible with this protocol and furnished various oxidative cyclization products **86** in moderate to excellent yields. This transformation could be scaled up without apparent loss of yield. Control experiments suggested a radical process and the fluorescence spectra showed that an excited Breslow intermediate was generated during the photooxidation process.

Mechanistically, the interaction of NHC **26** with aldehyde **85** generates the Breslow intermediate **87**, which can be promoted to excited state **88** under blue light. The following SET process between **88** and molecular oxygen furnishes radical pair species **89**. Subsequently,  $\alpha$ -amino radical **90** is formed by sequential 1,2-H shift and proton abstraction of **89**. Under iodide catalysis, this  $\alpha$ -amino radical can be further transformed into iminium species **92** *via*  $\alpha$ -iodoamine intermediate **91**. Then the oxidation of iminium by oxygen delivers radical cation **93**, which undergoes deprotonation to give zwitterionic radical **94**. After

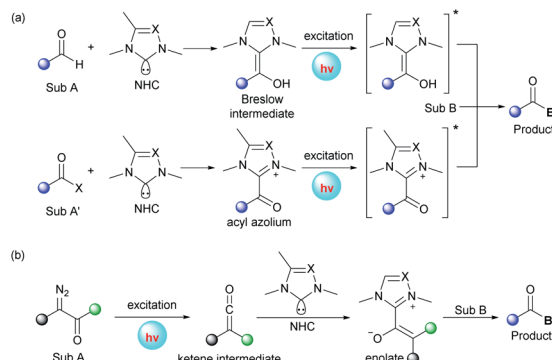
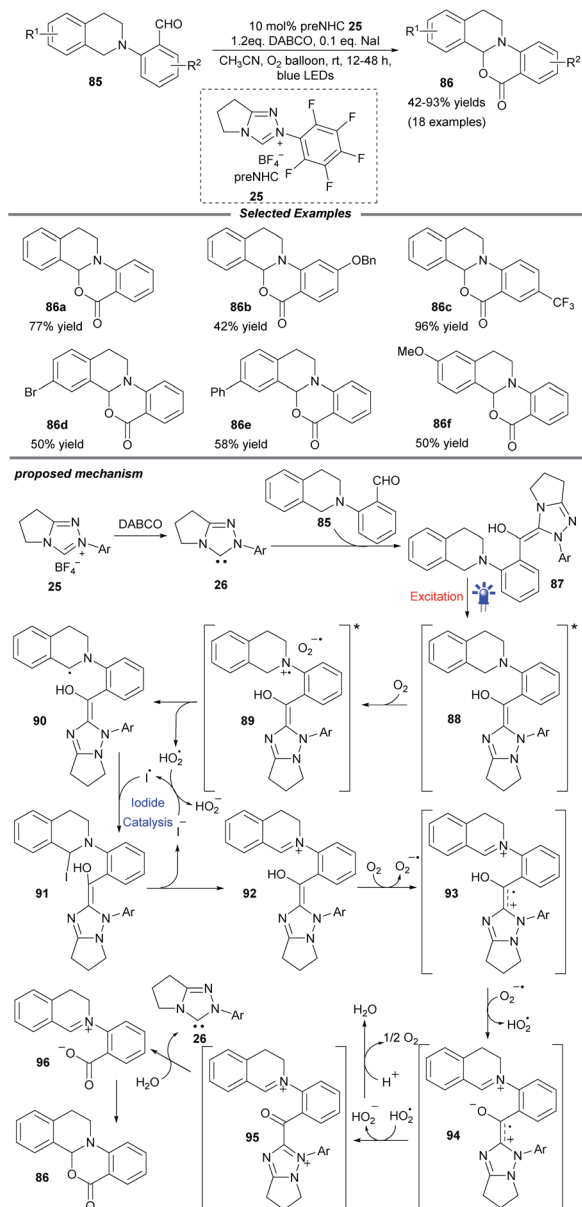


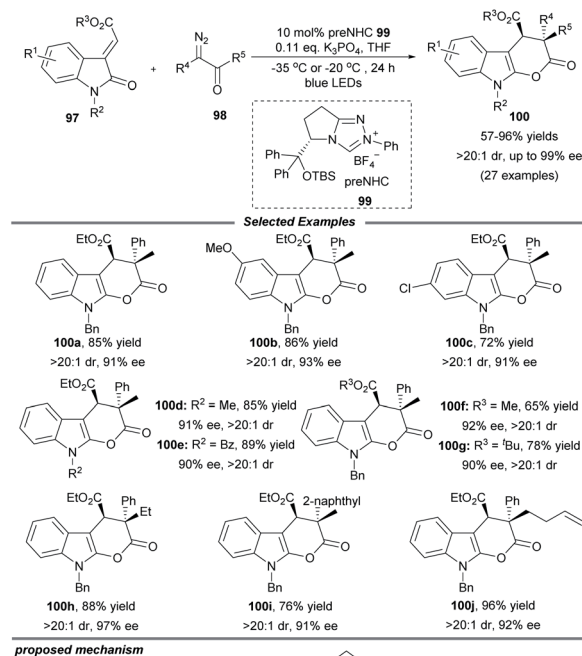
Fig. 2 Activation modes of photoexcited NHC-catalyzed transformations.



Scheme 9 NHC-catalyzed intramolecular cross dehydrogenative coupling.

further oxidation by the hydroperoxide radical, radical **94** is converted into acyl azolium intermediate **95**, which undergoes consecutive hydrolysis and deprotonation to reform NHC catalyst **26** and afford the iminium/carboxylate species **96**. A final intramolecular nucleophilic addition in **96** yields the cyclization product **86**.

The visible-light-driven Wolff rearrangement is an effective method for the conversion of readily available  $\alpha$ -diazo ketones into reactive ketenes.<sup>25</sup> Very recently, Hui and coworkers combined this photolytic process with NHC catalysis to realize an asymmetric [4 + 2] cycloaddition, affording a variety of chiral tetrahydropyrano[2,3-*b*]indoles in 57–96% yields with high diastereo- and enantioselectivity (Scheme 10).<sup>26</sup> The catalytic cycle begins with the photoactivation of  $\alpha$ -diazo ketones, which



Scheme 10 NHC-catalyzed stereoselective [4 + 2] cycloaddition.

can promote the Wolff rearrangement to generate ketene **101**. This reactive intermediate is then attacked by NHC catalyst **102** to form enolate species **103**. The following stereoselective [4 + 2] cycloaddition of **103** with 3-alkylenyloxindole gives the ion pair **104**, which delivers the final cyclization product with elimination of the active NHC catalyst **102**. Notably, a similar photochemical transformation was also realized by Song and coworkers with the use of a chiral isothioureia catalyst.<sup>25c</sup>

## 4. Conclusion and perspectives

In summary, a variety of successful transformations have undoubtedly demonstrated that the combination of visible-light photocatalysis and photoactivation with NHC catalysis provides a unique and efficient strategy for accessing valuable structural motifs from simple starting materials. This cooperative strategy can usually provide unique reaction pathways compared with classic two-electron NHC catalysis, thus expanding the application of NHC catalysis in modern organic synthesis. Moreover, high reaction selectivity, substrate diversity and functional group tolerance are enabled because of the mild reaction conditions.



Despite this impressive progress, the development of photochemical NHC catalysis is still in its infancy. There is still some significant potential to be exploited. First, there are only two reports regarding asymmetric catalysis systems. Broadly applicable, enantioselective transformations with high levels of regio- and enantio-control are awaited. Second, the transformations discussed above are mainly focused on the construction of carbon-carbon and carbon-oxygen bonds, and other reactions to forge carbon-heteroatom bonds (C-N, C-P, C-S, C-Si and so on) are still unexplored. Third, in-depth experimental and theoretical studies are highly desirable to help chemists design and discover novel chemical transformations, as well as new catalysts or catalyst systems. Ultimately, we deeply believe that the collaborative photo/NHC catalysis strategy will evolve into a practical synthetic tool in the construction of natural products and pharmaceuticals. We hope that this review will inspire more research efforts and further investigations in this intriguing and emerging area.

## Conflicts of interest

There are no conflicts to declare.

## Acknowledgements

We are grateful to the National Science Foundation of China (No. 21822103, 21820102003, 21772052, 21772053 and 91956201), the Program of Introducing Talents of Discipline to Universities of China (111 Program, B17019), the Natural Science Foundation of Hubei Province (2017AHB047) and the International Joint Research Center for Intelligent Biosensing Technology and Health for support of this research.

## Notes and references

- 1 F. E. Hahn and M. C. Jahnke, *Angew. Chem., Int. Ed.*, 2008, **47**, 3122–3172.
- 2 J. Chen and Y. Huang, *N-Heterocyclic Carbenes as Brønsted Base Catalysts*, Wiley-VCH, 2018, ch. 9, pp. 261–286.
- 3 For selected reviews, see: (a) X. Bugaut and F. Glorius, *Chem. Soc. Rev.*, 2012, **41**, 3511–3522; (b) X.-Y. Chen and S. Ye, *Org. Biomol. Chem.*, 2013, **11**, 7991–7998; (c) M. N. Hopkinson, C. Richter, M. Schedler and F. Glorius, *Nature*, 2014, **510**, 485–496; (d) D. M. Flanigan, F. Romanov-Michailidis, N. A. White and T. Rovis, *Chem. Rev.*, 2015, **115**, 9307–9387; (e) M.-H. Wang and K. A. Scheidt, *Angew. Chem., Int. Ed.*, 2016, **55**, 14912–14922; (f) X.-Y. Chen, Z.-H. Gao and S. Ye, *Acc. Chem. Res.*, 2020, **53**, 690–702; (g) Q. Zhao, G.-R. Meng, M. Szostak and S. P. Nolan, *Chem. Rev.*, 2020, **120**, 1981–2048.
- 4 For a recent review, see: T. Ishii, K. Nagao and H. Ohmiya, *Chem. Sci.*, 2020, **11**, 5630–5636.
- 5 (a) I. Nakanishi, S. Itoh, T. Suenobu, H. Inoue and S. Fukuzumi, *Chem. Lett.*, 1997, **26**, 707–708; (b) I. Nakanishi, S. Itoh, T. Suenobu and S. Fukuzumi, *Chem. Commun.*, 1997, 1927–1928; (c) I. Nakanishi, S. Itoh, T. Suenobu and S. Fukuzumi, *Angew. Chem., Int. Ed.*, 1998, **37**, 992–994; (d) I. Nakanishi, S. Itoh and S. Fukuzumi, *Chem.-Eur. J.*, 1999, **5**, 2810–2818.
- 6 J. Guin, S. D. Sarkar, S. Grimme and A. Studer, *Angew. Chem., Int. Ed.*, 2008, **47**, 8727–8730.
- 7 (a) N. A. White and T. Rovis, *J. Am. Chem. Soc.*, 2014, **136**, 14674–14677; (b) N. A. White and T. Rovis, *J. Am. Chem. Soc.*, 2015, **137**, 10112–10115.
- 8 (a) Y. Du, Y.-H. Wang, X. Li, Y.-L. Shao, G.-H. Li, R. D. Webster and Y. R. Chi, *Org. Lett.*, 2014, **16**, 5678–5681; (b) Y.-X. Zhang, Y. Du, Z.-J. Huang, J.-F. Xu, X.-X. Wu, Y.-H. Wang, M. Wang, S. Yang, R. D. Webster and Y. R. Chi, *J. Am. Chem. Soc.*, 2015, **137**, 2416–2419; (c) B.-S. Li, Y.-H. Wang, R. S. J. Proctor, Y.-X. Zhang, R. D. Webster, S. Yang, B.-A. Song and Y. R. Chi, *Nat. Commun.*, 2016, **7**, 12933–12940; (d) X.-X. Wu, Y.-X. Zhang, Y.-H. Wang, J. Ke, M. Jeret, R. N. Reddi, B.-A. Song and Y. R. Chi, *Angew. Chem., Int. Ed.*, 2017, **56**, 2942–2946.
- 9 X.-Y. Chen, K.-Q. Chen, D.-Q. Sun and S. Ye, *Chem. Sci.*, 2017, **8**, 1936–1941.
- 10 (a) T. Ishii, Y. Kakeno, K. Nagao and H. Ohmiya, *J. Am. Chem. Soc.*, 2019, **141**, 3854–3858; (b) T. Ishii, K. Ota, K. Nagao and H. Ohmiya, *J. Am. Chem. Soc.*, 2019, **141**, 14073–14077; (c) K. Ota, K. Nagao and H. Ohmiya, *Org. Lett.*, 2020, **22**, 3922–3925.
- 11 For selected reviews, see: (a) J. M. R. Narayanam and C. R. J. Stephenson, *Chem. Soc. Rev.*, 2011, **40**, 102–113; (b) J. Xuan and W.-J. Xiao, *Angew. Chem., Int. Ed.*, 2012, **51**, 6828–6838; (c) C. K. Prier, D. A. Rankic and D. W. C. MacMillan, *Chem. Rev.*, 2013, **113**, 5322–5362; (d) D. M. Schultz and T. P. Yoon, *Science*, 2014, **343**, 1239176; (e) M. Peña-López, A. Rosas-Hernández and M. Beller, *Angew. Chem., Int. Ed.*, 2015, **54**, 5006–5008; (f) N. A. Romero and D. A. Nicewicz, *Chem. Rev.*, 2016, **116**, 10075–10166; (g) Q.-Q. Zhou, Y.-Q. Zou, L.-Q. Lu and W.-J. Xiao, *Angew. Chem., Int. Ed.*, 2019, **58**, 1586–1604; (h) Y. Wei, Q.-Q. Zhou, F. Tan, L.-Q. Lu and W.-J. Xiao, *Synthesis*, 2019, **51**, 3021–3054.
- 12 A. Galván, F. J. Fañanás and F. Rodríguez, *Eur. J. Inorg. Chem.*, 2016, 1306–1313.
- 13 For selected reviews, see: (a) M. N. Hopkinson, B. Sahoo, J.-L. Li and F. Glorius, *Chem.-Eur. J.*, 2014, **20**, 3874–3886; (b) K. L. Skubi, T. R. Blum and T. P. Yoon, *Chem. Rev.*, 2016, **116**, 10035–10074; (c) J. Twilton, C. Le, P. Zhang, M. H. Shaw, R. W. Evans and D. W. C. MacMillan, *Nat. Rev. Chem.*, 2017, **1**, 0052–0070.
- 14 D. A. DiRocco and T. Rovis, *J. Am. Chem. Soc.*, 2012, **134**, 8094–8097.
- 15 E. Yoshioka, M. Inoue, Y. Nagoshi, A. Kobayashi, R. Mizobuchi, A. Kawashima, S. Kohtani and H. Miyabe, *J. Org. Chem.*, 2018, **83**, 8962–8970.
- 16 Z.-H. Xia, L. Dai, Z.-H. Gao and S. Ye, *Chem. Commun.*, 2020, **56**, 1525–1528.
- 17 (a) A. Arefolov and J. S. Panek, *J. Am. Chem. Soc.*, 2005, **127**, 5596–5603; (b) P. Cheruku, J. L. Keffer, C. Dogo-Isonagie and C. A. Bewley, *Bioorg. Med. Chem. Lett.*, 2010, **20**, 4108–4111; (c) W. Schmidt, T. M. Schulze, G. Brasse, E. Nagrodzka, M. Maczka, J. Zettel, P. G. Jones,





- J. Grunenberg, M. Hilker, U. Trauer-Kizilelma, U. Braun and S. Schulz, *Angew. Chem., Int. Ed.*, 2015, **54**, 7698–7702.
- 18 W. Yang, W.-M. Hu, X.-Q. Dong, X. Li and J.-W. Sun, *Angew. Chem., Int. Ed.*, 2016, **55**, 15783–15786.
- 19 L. Dai, Z.-H. Xia, Y.-Y. Gao, Z.-H. Gao and S. Ye, *Angew. Chem., Int. Ed.*, 2019, **58**, 18124–18130.
- 20 L. Dai and S. Ye, *Org. Lett.*, 2020, **22**, 986–990.
- 21 A. V. Davies, K. P. Fitzpatrick, R. C. Betori and K. A. Scheidt, *Angew. Chem., Int. Ed.*, 2020, **59**, 9143–9148.
- 22 For selected reviews, see: (a) T. Bach and J. P. Hehn, *Angew. Chem., Int. Ed.*, 2011, **50**, 1000–1045; (b) D. Ravelli, S. Protti and M. Fagnoni, *Chem. Rev.*, 2016, **116**, 9850–9913; (c) J. A. Dantas, J. T. M. Correia, M. W. Paixão and A. G. Corrêa, *ChemPhotoChem*, 2019, **3**, 506–520.
- 23 A. Mavroskoufis, K. Rajes, P. Golz, A. Agrawal, V. Ruß, J. P. Götze and M. N. Hopkinson, *Angew. Chem., Int. Ed.*, 2020, **59**, 3190–3194.
- 24 Z.-H. Gao, Z.-H. Xia, L. Dai and S. Ye, *Adv. Synth. Catal.*, 2020, **362**, 1819–1824.
- 25 For selected examples, see: (a) M.-M. Li, Y. Wei, J. Liu, H.-W. Chen, L.-Q. Lu and W.-J. Xiao, *J. Am. Chem. Soc.*, 2017, **139**, 14707–14713; (b) Y. Wei, S. Liu, M.-M. Li, Y. Li, Y. Lan, L.-Q. Lu and W.-J. Xiao, *J. Am. Chem. Soc.*, 2019, **141**, 133–137; (c) T. Fan, Z.-J. Zhang, Y.-C. Zhang and J. Song, *Org. Lett.*, 2019, **21**, 7897–7901; (d) J. Meng, W.-W. Ding and Z.-Y. Han, *Org. Lett.*, 2019, **21**, 9801–9805; (e) Q.-L. Zhang, Q. Xiong, M.-M. Li, W. Xiong, B. Shi, Y. Lan, L.-Q. Lu and W.-J. Xiao, *Angew. Chem., Int. Ed.*, 2020, **59**, 14096–14100; (f) M.-M. Li, Q. Xiong, B.-L. Qu, Y.-Q. Xiao, Y. Lan, L.-Q. Lu and W.-J. Xiao, *Angew. Chem., Int. Ed.*, 2020, DOI: 10.1002/anie.202006366.
- 26 C.-Y. Wang, Z.-Y. Wang, J. Yang, S.-H. Shi and X.-P. Hui, *Org. Lett.*, 2020, **22**, 4440–4443.

